This is the manuscript version before submission to peer-review. The final version of the manuscript can be found at the publisher, by following the link:

http://onlinelibrary.wiley.com/doi/10.1002/chem.201600962/full
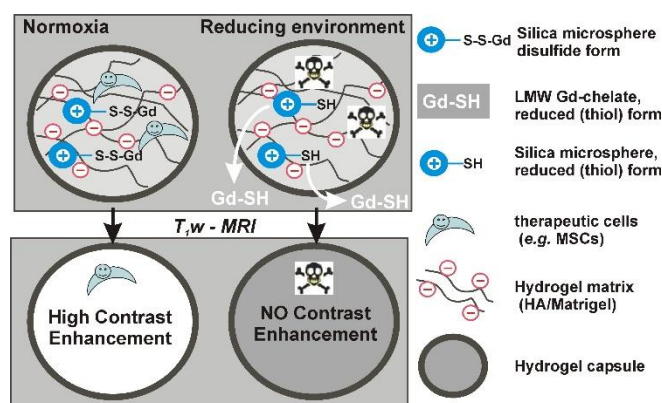
COMMUNICATION

Gadolinium-decorated silica microspheres as redox-responsive MRI probes for applications in cell therapy follow-up

M. Muñoz Úbeda,[a,†] F. Carniato,[a,†] V. Catanzaro,[a,d] S. Padovan,[b] C. Grange,[c] S. Porta,[d] C. Carrera,[d] L. Tei,[a] and G. Digilio[a,*]

Abstract: Silica microspheres have been decorated with Gd-HPDO3A-like complexes through a disulphide bond to obtain a redox-responsive MRI probe. This probe is designed to be interspersed with therapeutic cells within hydrogel capsules, to enable the longitudinal follow-up by MRI of the redox microenvironment surrounding the embedded cells.

Cell therapy can be broadly defined as the transplantation of living cells for the treatment of a wide number of medical disorders. Amongst therapeutic cells, Mesenchymal Stem Cells (MSCs) are those most often chosen for pre-clinical studies[1] as well as clinical trials because of efficacy, safety and lack of ethical issues. Although MSCs therapy is poised to establish a new clinical paradigm in regenerative medicine, studies completed so far have produced mixed results, with overall limited clinical benefits on the long term.[2] A major challenge to improve cell therapy is to enhance long term cell survival by escaping the host immune response. For cell therapy applications that require the *in situ* delivery of therapeutic cells (by open surgery or local infusion), a viable route to protect cell grafts from immune rejection can be the (micro)encapsulation of therapeutic cells within synthetic, bioabsorbable hydrogels with engineered extracellular matrix (ECM) properties.[3] This can provide a shield against recognition by either innate and adaptive response. In addition, mimicking a native environment around transplanted cells minimizes the detrimental effects due to abrupt microenvironment changes that follow transplantation. A typical hydrogel forming polymer for cell encapsulation is alginate, but several others are under investigation, including those based on collagen and hyaluronic acid (HA), whose mechanical and physico-chemical properties can be tailored to specific applications.[4] The cell encapsulation approach to deliver cell therapy offers the outstanding possibility to add imaging functionalities interspersed with therapeutic cells within the capsule, then to enable the longitudinal follow-up by imaging techniques of the artificial microenvironment surrounding the transplanted cells.[5] The basic idea is to incorporate imaging probes responsive to ECM properties that can be unambiguously linked to the capacity of the artificial microenvironment to support

cell survival. Extracellular pH (pH$_e$) has been demonstrated to decrease appreciably as a consequence of the events related to immune-rejection and death of grafted cells. Polyarginine-containing liposomes as pH$_e$-nanosensors for the CEST-MRI modality have been encapsulated with hepatocytes within alginate capsules and subcutaneously grafted in mice. The decrease of pH$_e$, as monitored by MRI, well correlated with the loss of encapsulated cells.[6] Redox microenvironment rather than pH$_e$ may represent a more suitable indicator to assess whether the graft is metabolically active or hypoxic. As a matter of facts, a key aspect in graft integration into the host is the ability of therapeutic cells to recruit a vascular supply of oxygen and nutrients to support long-term survival. If neovascularization fails, microenvironment hypoxia arises that is expected to correlate with poor cell survival. According to this view, we present the design, synthesis and characterization of a redox-responsive MRI probe to follow-up the redox microenvironment surrounding cells embedded within a hydrogel-based matrix. The redox responsive probe is composed of porous silica microspheres (SiMSs) whose surface has been decorated with *i)* a Gd-HPDO3A-like chelate through a disulfide bond, that provides responsivity to redox potential[7] (HPDO3A: 1,4,7-tris(carboxymethyl)-10-(2-hydroxypropyl)-1,4,7,10-tetraazacyclododecane); and *ii)* rhodamine B to allow for multimodal (optical) imaging. These particles are designed with size in the micrometer range to ensure a stable entrapment within the synthetic extracellular matrix. Within the planned application, Gd labelled SiMSs (shortly, Gd-SiMSs) interspersed with therapeutic cells should cause a bright contrast within the hydrogel phase in T_1-weighted MR images (Scheme 1). Responsivity to redox microenvironment is achieved by pharmacokinetic modulation: increasingly reducing conditions are expected to shift the disulphide/thiol redox equilibrium towards the thiol form,[8] ultimately resulting in the release of the low molecular weight Gd-chelate in the thiol form (Gd-SH; see Scheme 2). As Gd-SH is small and neutral, it is expected to

[a.] *Department of Science and Technologic Innovation, Università del Piemonte Orientale "Amedeo Avogadro", Viale T. Michel 11, I-15121 Alessandria, Italy. Email: giuseppe.digilio@uniupo.it*

[b.] *Institute for Biostructures and Bioimages (CNR) c/o Molecular Biotechnology Center Via Nizza 52, 10126 Torino, Italy.*

[c.] *Department of Medical Sciences, University of Turin, Via Nizza 52, 10126 Torino, Italy.*

[d.] *Department of Molecular Biotechnology and Health Science & Center for Molecular Imaging, University of Turin, Via Nizza 52, 10126 Torino, Italy.*

† These authors contributed equally to this work.

Scheme 1. Rationale for the use of Gd-SiMSs as redox-responsive MRI probes to follow-up the survival of encapsulated cells.
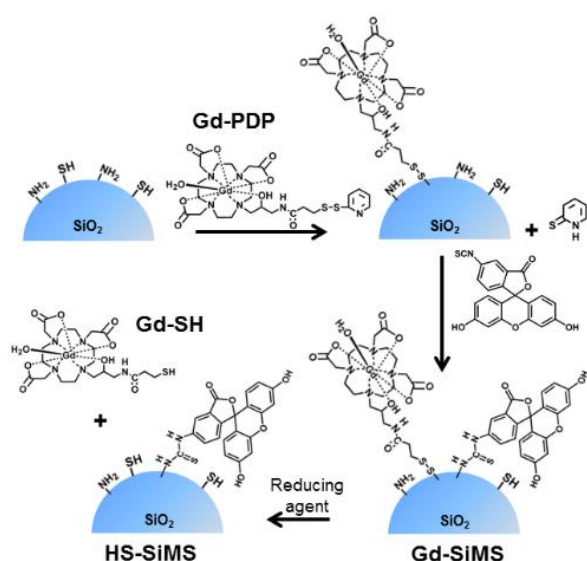
**Scheme 2.** Schematic view of the synthesis of bimodal redox-responsive silica microspheres (Gd-SiMS).
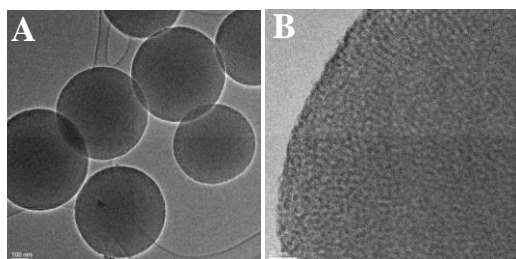
Figure 1. HR-TEM micrographs of SiMS at low (A) and high (B) magnifications.

diffuse out the hydrogel phase causing a progressive decrease of T_1 contrast enhancement.

Silica microspheres were prepared through a sol–gel synthesis, by adapting a procedure reported in the literature.[9] Particles with spherical shape and size of *ca.* 1 μm (as indicated by TEM micrographs, Fig. 1A) were obtained. Micrographs collected at higher magnifications (Fig. 1B) indicate the presence of a pore array, whose evidence is strengthened by N_2 physisorption analysis (Fig. S1). The sample shows a pore-size distribution with maximum at 5 nm and pores volume of 0.71 cm^3/g.

The silica surface was functionalized with amino and thiol groups, through simultaneous reaction of silica particles with aminopropyltriethoxysilane and mercaptopropyltrimethoxysilane in toluene suspension (see SI). A marked reduction of the pores volume of *ca.* 60% occurred as a consequence of the surface functionalization (Fig. S1). Functional groups are randomly distributed both inside the pores and on the external surface of silica particles. The presence of –NH$_2$ and –SH groups on silica surface was confirmed by the characteristic IR absorptions falling at 3370 and 3300 cm^{-1} (asymmetric and symmetric stretching mode of –NH$_2$ groups), and at 2570 cm^{-1} (stretching mode of –SH, Fig. S2). The amount of amino and thiol groups was 1.05 mmol/g and 0.39 mmol/g, respectively, as determined by CHNS
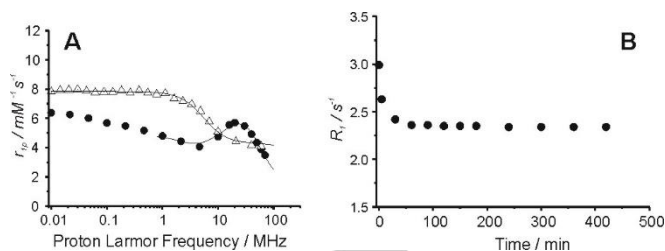
Figure 2. (**A**) 1H NMRD profiles of aqueous solutions of Gd-PDP (Δ) and Gd-SiMS (●) at 37 °C. The best-fit curves were calculated using the parameters of Table S1. (**B**) Kinetics of the reduction of the Gd-SiMS disulfide bond by TCEP ([Gd] = 0.4 mM; [TCEP] = 0.4 mM) followed by R_1 measurement at 20 MHz and 25°C.

elemental analysis. The bimodal Gd-SiMS system was then obtained following two consecutive synthetic steps (Scheme 2). The first one consists on linking a Gd-chelate to the silica thiol groups with the formation of the redox-responsive disulfide. To this purpose, compound Gd-PDP bearing the thiol-reactive 2-pyridyl-dithio group was synthesized. This novel compound is based on the macrocyclic octadentate HPDO3A chelating cage, which ensures higher chemical inertness,[10a] higher catabolic stability[10b] and low cell penetrating potential[10c] as compared to available heptadentate DO3A complexes or linear complexes. The conjugation of Gd-PDP to the free thiols on the silica surface was carried out in water at RT for 4 hrs by monitoring the release of 2-pyridine-thione at 343 nm (molar absorptivity of 8081 M^{-1}cm^{-1}).[7a] The amount of Gd in the final material was estimated to be 0.04 mmol/g, as found by inductively coupled plasma optical emission spectrometry (ICP-OES) gadolinium analysis. The chemical linkage of rhodamine B isothiocyanate to a fraction of the –NH$_2$ functionalities located on the surface was performed in acetonitrile in the presence of *N,N*-Diisopropylethylamine. The amount of rhodamine B bound to the silica surface was 0.035 mmol/g, as estimated by UV/Vis spectroscopy (Fig. S3). After these conjugation reactions, particles with surface charge density of +10 mV in aqueous solution (data from Z-potential analysis), arising from surface free -NH$_3^+$, were obtained.

The electronic properties of the obtained bimodal silica microspheres (dubbed Gd-SiMSs) were investigated by UV/Vis and photoluminescence spectroscopy (Fig. S4). The UV/Vis spectrum of pure rhodamine in water shows an absorption maxima typical of π→π* transitions (λ = 530 and 562 nm).[11] The same bands are also found after dye coupling to silica surface, although slightly shifted to higher wavelengths and with a different intensity ratio as a consequence of a different chemical environment. The PL spectra of the free dye and the conjugated system display an emission band with a maximum at 577 and 583 nm, respectively (Fig. S4).

The relaxation properties of Gd-SiMSs were studied by recording the 1H nuclear magnetic relaxation dispersion (NMRD) profile in the frequency range 0.01 to 70 MHz at 37 °C (Fig. 2A). NMRD profiles report water proton relaxation rates R_1 (R_1=1/T_1) as a function of the magnetic field strength. To avoid particle sedimentation (at least for 24 hrs; Fig. S5), Gd-SiMSs were

suspended in aqueous xanthan gum (0.1 wt%). The ^{1}H NMRD profile of Gd-SiMSs show a broad relaxivity peak centered at about 20-30 MHz (r_1 = 5.7 mM^{-1}s^{-1} per Gd ion at 20 MHz), followed by a relaxivity dispersion at higher fields. This is typical of slowly tumbling macromolecular systems.[12] The NMRD profile was fitted according to the conventional paramagnetic relaxation model (based on Solomon-Bloembergen-Morgan and Freed's theories)[13] implemented with the Lipari–Szabo model-free approach[14], that accounts for relatively fast local motions superimposed to the global, slow microparticle motion (characterized by correlation times τ_{RL} and τ_{RG} , respectively). Best fitting yields a τ_{RL} value of 8.9 ns. Such a value is significantly longer than that of the free Gd-chelate (τ_R = 80 ps) indicating a slowing down of re-orientation dynamics, but the order parameter S^2=0.62 also indicates that there is a significant decoupling between global and local motions (full fitting parameters are available in SI). This is due to the flexibility of the linker connecting the Gd-chelate to the particle surface. As a result of unrestricted local flexibility, the NMRD relaxivity peak has a low amplitude. At 20 MHz and 37°C the relaxivity of Gd-SiMSs is 30% higher than that of the precursor Gd-PDP. On the other hand, except for the magnetic field range corresponding to the relaxivity peak, the NMRD profile of Gd-SiMSs shows somewhat lower relaxivities than Gd-PDP. This is likely due to the fact that a fraction of the Gd-chelates is located within particle pores, where the relaxivity is limited by poor water diffusion. In this regard, Gd-SiMS is very similar to other Gd-decorated mesoporous silicas reported in the literature.[15]

To assess the responsivity of the MRI probe to reducing agents, tris(2-carboxyethyl)phosphine (TCEP) was added to a suspension of Gd-SiMSs at neutral pH and the longitudinal relaxation rate was monitored over time at 20 MHz and 25 °C (Fig. 2B). At this magnetic field, the reductive cleavage of the disulfide bond can be followed by the 30% change of relaxivity due to the loss of the macromolecule effect ongoing from the Gd-SiMS to the Gd-SH form. The kinetics of release of the free Gd-SH complex is comparable to that of other published disulphide-based Gd compounds [7b,c]. This rules out any steric effect possibly interfering with the reductive cleavage, such as poor accessibility of the disulphide bridge within silica pores.

To mimic the clearance of contrast from the synthetic tissue, Gd-SiMSs were suspended into 1% agar and the gel was kept in contact under gentle shaking with a 200-fold excess volume of buffer (see SI Scheme S1). Such buffer contained or not 50 mM GSH. Axial T$_1$w-MR images were taken at several time points across the agar phase (Fig. 3). In the presence of GSH, the reductive cleavage of the disulfide bond and clearance of Gd-SH from the agar phase into the buffer took place, leading to the almost complete drop of signal enhancement in the agar phase, as expected.

The biocompatibility has been assessed by incubating hMSCs with Gd-SiMSs up to 12 days and by evaluating cell viability, proliferation rate and morphology. Adverse effects were found at a particle-to-cell ratio of 6.6 ng$_{Gd-SiMS}$/cell, together with a significant particle uptake into the cytoplasm. Despite the large
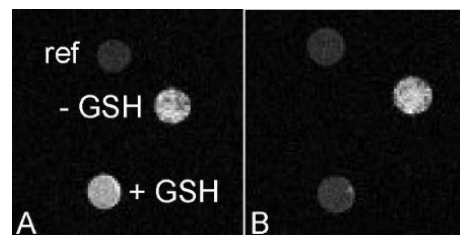
Figure 3. T$_1$w MRI at 7 T (300 MHz) of Gd-SiMSs suspended in agar phantoms before (**A**) and after 7-days washings (**B**) with a buffer containing (+ GSH) or not glutathione (- GSH). The agar phantom without Gd-SiMSs is labelled "ref".
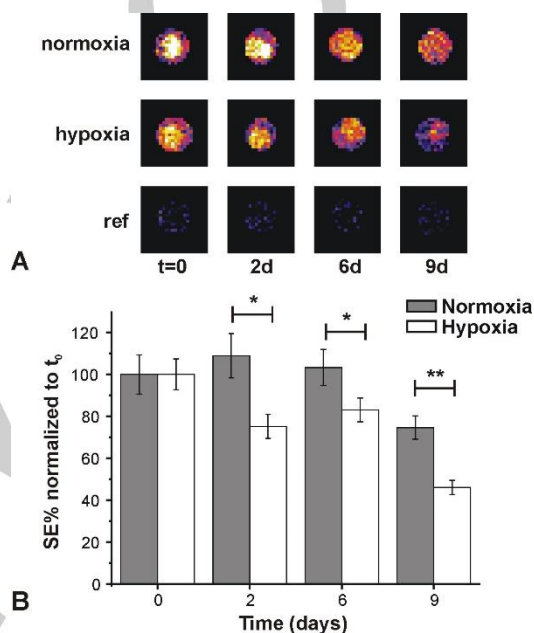
Figure 4. False color parametric images obtained from T$_1$w MRI at 7 T (300 MHz). (**A**) Signal Enhancement maps normalized by the SE at t=0 (SE%) of a phantom containing Gd-SiMSs/HA interspersed with hMSCs within a matrigel matrix under normoxia or reducing conditions. Each well was incubated in conditions that allow for the diffusion of the Gd-SH complex out of the hydrogel phase. The phantom labelled "ref" contains HA/Matrigel only (no Gd, no cells). (**B**) Time-evolution of the normalized SE with incubation time (days) as calculated from T$_1$w MR images (error bars are SEM over three slices; the asterisks indicate statistical significance according to the Student t-test).

particle size (*ca.* 1 μm), internalization still occurs because of the slight cationic charge of particles. However, pre-mixing of Gd-SiMSs with strongly anionic HA (1:1 w/w) to shield excess positive charge and dispersion of the Gd-SiMS/HA system with hMSC within a gelatin-based hydrogel (BD Matrigel^{TM}) abolished adverse effects up to a particle-to-cell ratio of 40 ng$_{Gd-SiMS}$/cell, while providing a stable labelling of the synthetic extracellular microenvironment.

Finally, Gd-SiMS were assessed for their ability to report about the extracellular redox microenvironment within a gelatin/HA hydrogel embedding hMSCs. Cells were interspersed with Gd-SiMSs within the hydrogel at a cell density of 400 cells/μL, particle-to-cell ratio of 30 ng$_{Gd-SiMS}$/cell, and total Gd concentration of 50 μM. The cell-embedding hydrogel (100 μL) was kept in contact with 150 μL of culture medium and incubated at 37°C

under conditions simulating either a normoxic or a highly reducing extracellular microenvironment (hypoxia and 30 mM reduced glutathione). Such a two-phase system (see SI Scheme S2) was conceived as a the simplest way to mimic clearance of reduced Gd-SH from the hydrogel phase, that is strictly needed to achieve the pharmacokinetic modulation of the signal enhancement as sketched in Scheme 1. T_1w MR images at 7 T were taken across the hydrogel phase at regular time intervals over 9 days. Signal intensities within MR images were transformed into Signal Enhancements (SE) with reference to the Gd-free HA/collagen hydrogel and normalized to the SE obtained at t=0 (Fig. 4). The parametric images show that the SE% drop in the reducing hydrogel becomes significantly higher than that of normoxia since day-2, and approaches 54% at day 9 (note that 60% is the maximum drop achievable by our experiment design, see SI Scheme S2). The difference in the signal drop is maintained throughout the whole experiment duration, even though some drop of the absolute SE% is noted also for the normoxia hydrogel at endpoint day-9. This is likely due to remodeling/degradation of the gelatin matrix, that creates time-fluctuating, heterogeneous spots of Gd-SiMS aggregation within the hydrogel (see Fig. 4A). This is a source of experimental uncertainty of SE measurements. Cell viability was evaluated at day-9 by the assessment of the proliferation and morphology of cells within the hydrogels. Live cells were found in the normoxia hydrogel, but not in the reducing one (Fig. S6). Thus, it is concluded that the assessment of the extracellular redox state as a marker of its capacity to sustain cell survival cannot rely on measurements at a single time point. Instead, the persistency of high redox potential along an extended period of time is a more reliable indicator of progressive cell loss.

In conclusion, this work shows for the first time the application of redox-responsive, silica based microparticles as MRI probes for the longitudinal follow-up of the redox microenvironment within an artificial extracellular matrix. The next step prior to proceed to *in vivo* studies deals with the optimization of Gd-SIMS surface properties to minimize time-dependent particle aggregation driven by hydrogel remodeling, to enhance both biocompatibility and sensitivity. This can be pursued, for instance, by decorating the particle surface with polyethylene glycol chains and/or by fine tuning of particle surface charge.

Experimental Section

Synthesis of SiMS and derived materials: SiMS particles were prepared through a sol-gel procedure, calcined in air and functionalized with aminopropyl (25 wt%) and 3-Mercaptopropyl-alkoxysilanes (25 wt%) in toluene. Finally, the surface of the organo-modified sample was decorated with a Gd-HPDO3A-like complex and rhodamine B isothiocyanate. MR images were acquired with a Bruker Avance microimaging MR scanner operating at 7T. Further experimental details are available online.

Acknowledgements

1 *a)* C. Grange, A. Moggio, M. Tapparo, S. Porta, G. Camussi, and B. Bussolati, *Physiol. Rep.* **2014**, *2*,e12009; *b)* M.B. Herrera, B. Bussolati, S. Bruno, V. Fonsato, G.M. Romanazzi, and G. Camussi, *Int. J. Mol. Med.*, **2004**, *14*, 1035-1041; *c)* B. Bussolati, and G. Camussi, *Contrib. Nephrol.*, **2007**, *156*, 250-258.

2 J. Ankrum and J.M. Karp, *Trends in Molecular Medicine*, **2010**, *16*, 203-209.

3 *a)* A. Goren, N. Dahan, E. Goren, L. Baruch, and M. Machluf, *FASEB J.*, **2010**, *24*, 22-31; *b)* R. Katare R, F. Riu, J. Rowlinson, A. Lewis, R. Holden, M. Meloni, C. Reni, C. Wallrapp, C. Emanueli and P. Madeddu, *Arterioscler. Thromb. Vasc. Biol.*, **2013**, *33*, 1872-80; *c)* B.P. Barnett, A. Arepally, P.V. Karmarkar, D. Qian, W.D. Gilson, P. Walczak, V. Howland, L. Lawler, C. Lauzon, M. Stuber, D.L. Kraitchman and J.W.M. Bulte, *Nature Med.*, **2007**, *13*, 986-991.

4 *a)* R.M. Hernández, G. Orive, A. Murua and J.L. Pedraz, *Adv. Drug Delivery Reviews* **2010**, *62*, 711-730; *b)* G.D. Prestwich, *J. Controlled Release* **2011**, *155*, 193-199.

5 A.V. Naumova, M. Modo, A. Moore, C.E. Murry and J.A. Frank, *Nat biotechnology*, **2014**, *32*, 804-818; *b)* A.K. Srivastava, D.K. Kadayakkara, A. Bar-Shir, A.A. Gilad, M.T. McMahon and J.W.M. Bulte, *Disease Models & Mechanisms*, **2015**, *8*, 323-336.

6 K.W.Y. Chan, G. Liu, X. Song, H. Kim, T. Yu, D.R. Arifin, A.A. Gilad, J. Hanes, P. Walczak, P.C.M. van Zijl, J.W.M. Bulte and M.T. McMahon *Nat Materials,* **2013**, *12*, 268-275.

7 *a)* C. Carrera, G. Digilio, S. Baroni, D. Burgio, S. Consol, F. Fedeli, D. Longo, A. Mortillaro and S. Aime, *Dalton Trans.* **2007**, 4980-4987. *b)* E. Terreno, C. Boffa, V. Menchise, F. Fedeli, C. Carrera, D. Delli Castelli, G. Digilio and S. Aime*, Chem. Commun.*, **2011**, *47*, 4667-4669. *c)* J. Martinelli, M. Fekete, L. Tei and M. Botta *Chem. Commun.*, **2011**, *47*, 3144-3146. *d)* J. Martinelli, K. Thangavel, L. Tei, M. Botta, *Chem Eur. J.*, **2014**, *20*, 10944-10952; *e)* C. Gløgård, G. Stensrud and S. Aime, *Magn. Reson. Med.*, **2003**, *41*, 585-588; *f)* Q.N. Do, J.S. Ratnakar, Z. Kovacs and A.D. Sherry, *ChemMedChem* **2014**, *9*, 1116-1129. *g)* P.B. Tsitovich, P.J. Burns, A.M. McKay, J.R. Morrow, *J. Inorg. Biochem.,* **2014**, *133*, 143-154.

8 *a)* R. Banerjee, *J. Biol. Chem.* **2012**, *287*, 4397-4402. *b)* F.Q. Schafer and G.R. Buettner, *Free Rad. Biol. Med.*, **2001**, *30*, 1191-1212. *c)* V. Menchise, G. Digilio, E. Gianolio, E. Cittadino, V. Catanzaro, C. Carrera and S. Aime *Mol. Pharmaceutics* **2011**, *8*, 1750-1756. *d)* B. Jagadish, G.P. Guntle, D. Zhao, V. Gokhale, T. J. Ozumerzifon, A.M. Ahad, E.A. Mash, N. Raghunand, *J. Med. Chem.*, **2012**, *55*, 10378–10386 ‖

9 W. Pan, J. Ye, G. Ning, Y. Lin, J. Wang, *Materials Research Bulletin*, **2009**, *44*, 280-283.

10 *a)* Z. Baranyai, Z. Pálinkás, F. Uggeri, A. Maiocchi, S. Aime and E. Brücher *Chem. Eur. J.* **2012**, 18, 16426–16435. *b)* E. Di Gregorio, E. Gianolio, R. Stefania, G. Barutello, G. Digilio and S. Aime, *Anal. Chem.*, **2013**, *85*, 5627-5631; *c)* G. Digilio, V. Menchise, E. Gianolio, V. Catanzaro, C. Carrera, R. Napolitano, F. Fedeli and S. Aime, *J. Med. Chem.* **2010**, *53*, 4877-4890.

11 F. Carniato, L. Tei, S. Phadngam, C. Isidoro, M. Botta, *ChemPlusChem*, **2015**, *80*, 503-510.

12 M. Botta, L. Tei, *Eur. J. Inorg. Chem.* **2012**, *12*, 1945-1960.

13 A. Merbach, L. Helm, E. Toth, The Chemistry of Contrast Agents in Medical Magnetic Resonance Imaging, 2nd ed., John Wiley & Sons, New York, **2013**

14 *a)* G. Lipari, S. Szabo, *J. Am. Chem. Soc.*, **1982**, *104*, 4546-4559; *b)* G. Lipari, S. Szabo, *J. Am. Chem. Soc.*, **1982**, *104*, 4559-4570.

15 *a)* F. Carniato, L. Tei, W. Dastrù , L. Marchese and M. Botta. *Chem. Commun.*, **2009**, *10*, 1246-1248. *b)* F. Carniato, L. Tei, M. Cossi, L. Marchese, M. Botta, *Chem. Eur. J.*, **2010**, *16*, 10727-10734.

WILEY-VCH

Entry for the Table of Contents

Layout 1:

COMMUNICATION

Silica microspheres have been decorated with Gd-HPDO3A-like complexes through a disulphide bond to obtain a redox-responsive MRI probe. This probe is designed to be interspersed with therapeutic cells within hydrogel capsules, to enable the longitudinal follow-up by MRI of the redox microenvironment surrounding the embedded cells.
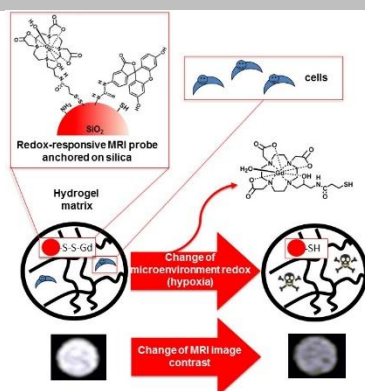
M. Muñoz Úbeda, F. Carniato, V. Catanzaro, S. Padovan, C. Grange, S. Porta, C. Carrera, L. Tei, G. Digilio*

Page No. – Page No.

Gadolinium-decorated silica microspheres as redox-responsive MRI probes for applications in cell therapy follow-up